

## Howieite, a New Type of Chain Silicate

H. R. WENK

Department of Geology and Geophysics, University of California at Berkeley

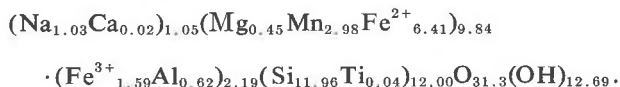
### Abstract

Howieite, one of the new iron silicate minerals from the Franciscan formation, represents a new type of chain silicate, hybrid between a single and a double chain. In effect, a four-octahedron-wide ribbon of the octahedral layer of mica is sandwiched between two hybrid  $[\text{Si}_6\text{O}_{17}]$ -chains. As for the tetrahedral sheets in mica, the apical oxygens of these chains face (and are shaped by) this ribbon. The resultant structural units run parallel to  $z$ , their flat sides being parallel to  $(1\bar{2}0)$  in howieite, which is thus analogous to (001) in the sheet silicates. Where the flat sides of two such structural units are adjacent, the basal oxygens of their  $[\text{Si}_6\text{O}_{17}]$ -chains form the interstice that accommodates the large Na-atom. Those basal oxygens more distant from the Na-atom, and thus at the edges of the structural units, are shared by the octahedral ribbons of neighboring structural units. The structure was refined with 35 independent anisotropic atoms to an R-factor of 4.5 percent in space-group  $P\bar{1}$ . But partial order of divalent and trivalent ions on the 12 octahedral sites indicate that the true symmetry of howieite may be  $P1$ . The howieite structure could well be indicative of high pressures since it represents a much denser packing than in sheet silicates; thus its occurrence in the high-pressure, medium-temperature assemblages of the Franciscan formation is plausible from crystal chemical considerations.

### Introduction

Howieite is one of the three new silicate minerals which have recently been found in the riebeckite-stilpnomelane schists of the Franciscan formation in Northern California (Agrell *et al.*, 1965). The crystal used in the structure determination was collected at the type locality at Laytonville quarry (Mendocino County, California); it is a cleavage fragment from a plumose aggregate of black bladed crystals (Figure 1a) in carbonate-bearing stilpnomelane-riebeckite-spessartite-howieite-deerite<sup>1</sup> schist. Howieite is bi-axial negative ( $\alpha = 1.701$ ,  $\beta = 1.720$ ,  $\gamma = 1.734$ ,  $2V = 65^\circ$ ) with strong dispersion ( $v > r$ ) and pleochroism ( $\alpha$  golden,  $\gamma$  green). It is distinguished from the similar coexisting stilpnomelane by inclined extinction and higher birefringence. Howieite has two moderately good cleavages, (010) and (100). The density is 3.378 g/cc. The chemical formula

suggested by Agrell, Bown, and McKie (1965) is:



The following triclinic unit cell contains one formula unit:

$$a = 10.17(5) \text{ \AA}, \quad b = 9.72 \text{ \AA}, \quad c = 9.56 \text{ \AA}, \\ \alpha = 91.3^\circ, \quad \beta = 70.7^\circ, \quad \gamma = 109^\circ.$$

In the course of the structure determinations, both formula and lattice constants had only to be slightly modified. Howieite was an interesting choice for a structure determination because its lattice constants are different from any known silicates, and there is thus possibility of finding a new silicate structure type. Another stimulus was local reminiscence, since howieite was first discovered by Dr. Agrell of Cambridge University in the Berkeley mineralogy collection. The structure determination proved indeed that howieite possesses a new structure, intermediate between sheet and chain silicates. It can be described as a collapsed sheet silicate possibly indicative of the geological conditions of high pressure during metamorphic recrystallization in the Franciscan formation. Some basic features of the howieite structure have already been reported (Wenk, 1973).

<sup>1</sup> Deerite, another one of the three new minerals, has been described as belonging to space group  $P2_1/a$  with presence of submicroscopical twinning (Agrell *et al.*, 1965). Our precession and Laue photographs show diffraction spots whose equivalence in shape and intensity indicate that the mineral may rather possess the orthorhombic space group  $Pnma$  (62) ( $a = 18.885 \text{ \AA}$ ,  $b = 3.182 \text{ \AA}$  (needle axis),  $c = 10.337 \text{ \AA}$ ).

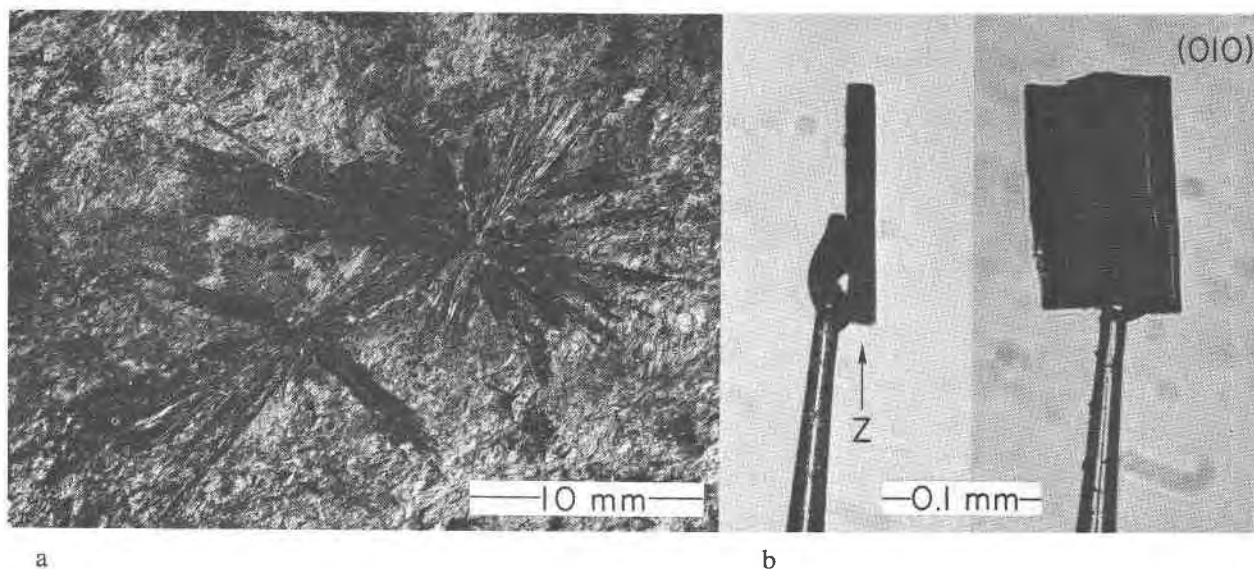


Fig. 1a. Plumose aggregate of howieite crystals in stilpnomelane-riebeckite schist.  
b. Prismatic bladed crystal, chosen for the structure determination.

## Experimental Procedures

### Material and Data Collection

Most howieite crystals were either bent, showed asterism, or consisted of several slightly disoriented domains. After examination by Laue photographs of many crystals on a precession camera, a small nearly perfect crystal ( $0.02 \times 0.1 \times 0.15$  mm) was found (Fig. 1b). This crystal was then oriented on a computer-controlled Picker diffractometer. Lattice constants and orientation angles were refined by least squares methods from positions of 12 independent reflections ( $a = 10.170(4)$  Å,  $b = 9.774(4)$  Å,  $c = 9.589(4)$  Å,  $\alpha = 91.22(5)^\circ$ ,  $\beta = 70.76(5)^\circ$ ,  $\gamma = 108.09(5)^\circ$ <sup>2</sup>. Intensity data were then collected on the four-circle diffractometer using  $\text{MoK}\alpha$  radiation with highly oriented graphite as monochromator in the  $\theta$ - $2\theta$  scan mode up to  $2\theta$  angles of  $60^\circ$ . A scan rate of  $1^\circ/\text{min}$  was used with a scan width of  $1.4^\circ + \Delta 2\theta$ , where  $\Delta 2\theta$  is the distance between calculated maxima for  $K\alpha_1$  and  $K\alpha_2$  peaks. Background was counted for 4 seconds stationary on either side of the peak. The stability of the crystal and the diffractometer was checked by measuring the  $02\bar{6}$ ,  $4\bar{2}0$ , and 150 reflections after every two hundred reflections. These reflections showed constant intensity within 1 to 2 percent throughout data collection. The data were then

corrected for Lorentz and polarization effects. Standard deviations  $\sigma$  of individual reflections were determined from counting statistics of integrated count and background. An additional error of  $p = 4$  percent of the net intensity was added to the standard deviation to avoid overweighting of intense reflections (Duesler and Raymond, 1971; Corfield, Doedens, and Ibers, 1967). Of 5322 reflections only 4047 reflections with intensity  $>3\sigma$  were used in the refinement.

The data crystal had maximum point-to-point distances of  $0.02 \times 0.10 \times 0.15$  mm and was mounted approximately along the  $z$  axis (Fig. 1b). The linear absorption coefficient is  $53 \text{ cm}^{-1}$ . The value of  $e^{-\mu t}$  ranged from a minimum of 0.6 to a maximum of 0.9 at  $2\theta = 0^\circ$  (the variation is somewhat higher than this for high angle reflections). The actual range of integrated transmission factors is smaller than this and no absorption correction was applied. As discussed later, errors caused by absorption mainly affected the anisotropic temperature factors, which show a strong elongation parallel to  $y$ .

### Solution of the Structure

The structure was determined using a combination of sign determination (program FASTAN; Main, Woolfson, and Germaine, unpublished), Patterson, Fourier (program FORDAP; Zalkin, unpublished), and least-squares (program NUCLS6; Busing, Martin,

<sup>2</sup> Estimated errors in the least significant digits are given in parentheses.

and Levy, 1962; modified by Ibers and Raymond) techniques. Scattering-factor tables of Cromer and Mann (1968) interpolated for 0.1 electron formal charge were used for all atoms. A correction for anomalous dispersion effects was applied to Fe using both  $\Delta f'$  and  $\Delta f''$  (Cromer, 1965). The scattering factors of Na and Fe ( $M$ ) were modified to take care of minor substitutions using the chemical analysis by Agrell *et al* (1965),  $[\text{Na}_{0.98}\text{Ca}_{0.02}]$ ,  $[\text{Fe}^{2+}_{0.53}\text{Mn}_{0.25}\text{Mg}_{0.04}\text{Fe}^{3+}_{0.13}\text{Al}_{0.05}]$ .

First a Patterson map was calculated. Its main feature is a strong maximum at  $u = 0, v = 0, w = 1/3$  which can be interpreted as a chain arrangement of atoms parallel to the  $z$ -axis with a repeat of  $1/3$  ( $3.2 \text{ \AA}$ ) that just about corresponds to an O-O distance. A second step was to compute Wilson statistics and use them to calculate normalized structure factors  $|E|$  for 400 strong reflections. Results of Wilson statistics indicate that a centrosymmetric structure is more probable (average  $|E| = 664$ ,  $|E| > 1 : 18\%$ ,  $|E| > 2 : 6.1\%$ ). Using program FASTAN, signs of 310  $E$ 's were determined and for one of several solutions the  $E$  map in space-group  $P\bar{1}$  showed strong peaks at  $1/2, 0, 0; 1/2, 0, 0.33; -0.19, 0.18, 0.06; -0.19, 0.18, 0.39$ , and weaker ones at  $0.12, 0.30, 0.12; 0.12, 0.30, 0.45; -0.11, -0.30, 0.20; 0.20, -0.15, 0.26$  (Fig. 2, old setting); these all agree with the Patterson map. Refining scale factors and atomic positions by least-squares, the  $R$ -value dropped to 48 percent. Using 1043 reflections ( $|F|^2 > 5\sigma$ ,  $2\theta < 35^\circ$ ) with unit weight and combining a one-cycle full-matrix least-squares refinement with a difference Fourier, more atoms were added after each cycle and the  $R$ -value reached 29 percent after 5 cycles. On the Fourier maps, chains of atoms parallel to  $z$  with a  $1/3$  repeat were apparent from the start. It was not possible to refine it any further. Therefore symmetry was lowered to  $P1$  starting out new with 9 heavy atoms which showed up consistently in Fourier maps, one of them fixed at  $1/2, 0, 0$ . This refinement was much better, and at an  $R$ -value of 18 percent the structure was essentially solved with 12  $M$ , 12 Si, 44 O, and 1 Na located. It appeared at this point that the sign determination program placed the center of symmetry at a pseudo-center Fe (2), and the origin was now fixed in the Na position (Figure 2). We mention this question of origin in some detail to demonstrate the grade of resolution of a sign determination program. The pseudo-center which has been determined at Fe (2) is surprisingly asymmetric!

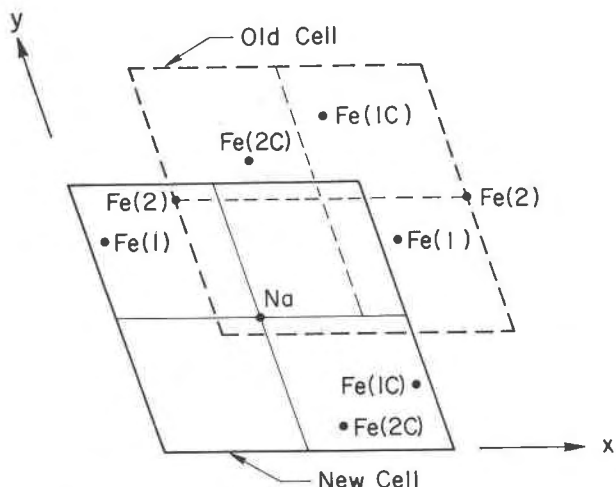


Fig. 2. Diagram indicating Fe(=M) positions and choice of unit cell in the beginning of the structure determination suggested by the sign determination program (dashed) and in the refined structure (solid).

### Refinement

At this stage a trial to define the structure in the centrosymmetric space-group  $P\bar{1}$  (averaging pseudosymmetrically related atoms) failed. The structure refined readily to  $R = 10$  percent in  $P1$  with 69 independent atoms. Now an attempt to use the centric space-group was successful, and final refinements were done with four models using 3721 independent reflections ( $|F_o| > 3\sigma$ ).

a) The first model assumed 35 independent atoms with isotropic temperature factors, refining 146 parameters (atomic positions, temperature factors  $B$ , a scale factor, an extinction coefficient [Zachariassen, 1968], and occupancy factors for  $M$  and Na atoms). The refinement converged after a few cycles (unweighted  $R = 6.13\%$ , weighted  $R = 7.79\%$ ). Final parameters from this refinement are listed in Tables 2 and 6 and occupancies in Figure 10. These data were used in the calculation of interatomic distances and bond angles in Tables 4-5 (with Program ORFFE).

b) An analogous refinement was done but with anisotropic temperature factors for all atoms, thus varying 321 parameters. This refinement also converged well (unweighted  $R = 4.55\%$ , weighted  $R = 6.18\%$ ). Atomic positions were identical to the isotropic refinement within less than the estimated error. Coefficients  $\beta_{ii}$  of the thermal ellipsoids are listed in Table 3. As can be seen, there is quite substantial anisotropy, particularly for the large Na atom (compare also Figure 7). A final difference

Fourier summation showed no peaks larger than  $+1.0 e/\text{\AA}^3$ , and  $-1.5 e/\text{\AA}^3$ , or roughly 10 percent of an oxygen atom. The largest peaks appeared near heavy atoms and are therefore interpreted as series termination ripples rather than any serious error in the final model (Figure 3). A list of  $F_o$ 's and  $F_c$ 's for this refinement is shown in Table 1.

c) The noncentric isotropic refinement (60 atoms with 288 parameters varied) converged slowly below  $R = 10$  percent and large correlation coefficients (up to 0.975) between parameters of pseudocentrosymmetrically related atoms were encountered. Estimated errors of the parameters were high, and after many cycles  $R$  (unweighted) reached 5.80 percent. Obviously the quality of the data set was insufficient to resolve the ambiguity as to whether howieite belongs to the  $P1$  or  $P\bar{1}$  space-group, and also least-squares methods do not lend themselves well to refining structures with a very strong pseudosymmetry. For other reasons, discussed below, we maintain that the true symmetry of howieite is  $P1$ .

d) In order to test the acentricity further in a model with fixed atomic positions and thermal parameters taken from the isotropic  $P\bar{1}$  refinement, the occupancies of the  $M$  sites were refined in  $P1$ . The refinement converged and showed significant differences between centrosymmetrically related sites, thus suggesting partial order of  $\text{Fe}^{2+}$ ,  $\text{Fe}^{3+}$ , Mg, and Al on the octahedral sites. Results are shown in Table 6 and Figure 8.

Another attempt at refining occupancy factors of  $M$  and octahedral O positions in  $P1$  also refined resulting in identical occupancies as in the former refinement (Table 6) and differences in atomic positions of centrosymmetrically related atoms of up to  $0.5 \text{\AA}$  (5 standard deviations).

For all these refinements (a-d), the extinction coefficient was very small ( $0 \pm 2 \times 10^{-8}$ ).

### Description of the Structure

The structure of howieite is displayed in Figures 4 and 5. An  $xy$  projection is easiest to visualize due to the formation of "chains" of all atoms parallel to the  $z$ -axis. Aiming at some natural order in the labeling of the 35 independent atoms, we used the repetition along the  $z$ -axis; for instance, O(2, 3) meaning the second oxygen atom on the third  $z$ -level. O(2, 3C) is its pseudocentrosymmetric counterpart.

$\text{SiO}_4$ -tetrahedra are linked to form rings of six, with the free corners of all of them pointing in the

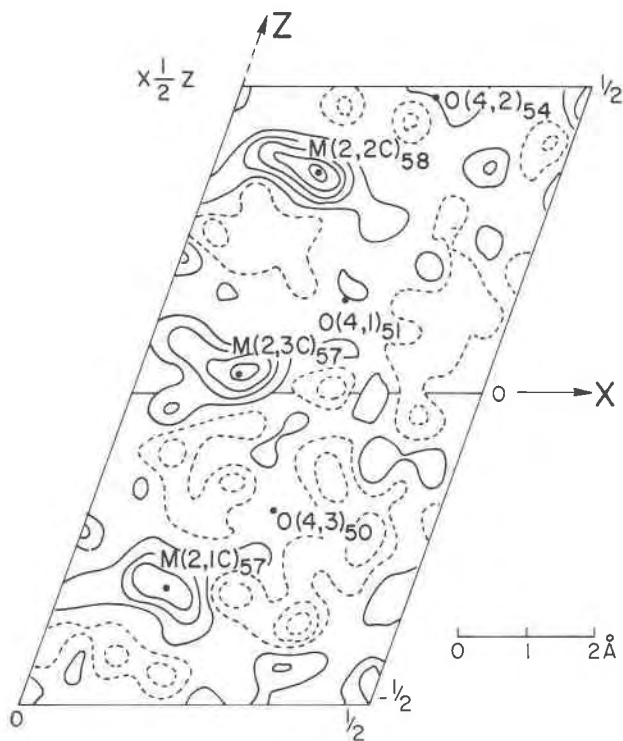


FIG. 3.  $x = 0.5z$  section of a difference Fourier based on the last anisotropic refinement cycle. The section contains the largest peak. Positions of close atoms are indicated. Contours are in  $1/10 e \text{\AA}^{-3}$ . Solid lines indicate positive, dashed lines indicate negative topography.

same direction. These six-membered rings are connected with one corner and extend as infinite garland-shaped chains parallel to the  $z$ -axis (Fig. 5). In the six-membered ring, two tetrahedra have three corners linked in the chain [Si(2)], four tetrahedra have only two [Si(1), Si(3)], thus forming a  $[\text{Si}_6\text{O}_{17}]$  unit which is a hybrid between a single and a double chain for which there is no representative so far. Si-O distances in the six independent tetrahedra are listed in Table 4. There is no significant difference in the average Si-O distance of the various sites (1.621–1.631 Å).

The tetrahedral chain is attached with corners to an octahedral band consisting of four rows of octahedra also extending parallel to the  $z$ -axis with a  $1/3 z$  repeat.  $M$ -O distances and  $O$ - $M$ -O angles (Table 5) are fairly uniform and show relatively little distortion. In this  $[\text{M}_{12}\text{O}_{30}]$  octahedral band: twelve oxygens—O(2, 1), O(2, 2), O(3, 2), O(3, 3), O(4, 1), O(4, 3) plus their centrosymmetric equivalents—are bonded to three  $M$  and one Si atoms; six oxygens—O(2, 3), O(3, 1), O(4, 2) plus equivalents—are only bonded to three  $M$  atoms; four oxygens—O(5, 1),



TABLE 1, continued

K	L	FO	FC	K	L	FO	FC	K	L	FO	FC	K	L	FO	FC	K	L	FO	FC	K	L	FO	FC								
-1	2	27	28	4	10	4	-3	-8	11	9	7	4	14	31	-3	5	17	8	7	3	61	64	-3	-9	37	36	-12	-4	14	14	
-1	3	27	28	9	6	18	11	-3	-7	11	15	7	5	31	31	-3	6	21	21	7	4	61	64	-3	-9	37	36	-12	-4	14	14
-1	4	17	18	9	7	10	16	-3	-4	43	41	7	7	60	57	-3	7	29	26	7	6	59	58	-3	-7	67	67	-12	-1	14	14
-1	5	13	12	9	8	37	37	-3	-6	32	37	7	8	18	19	-3	8	16	15	7	6	59	58	-3	-7	67	67	-12	-1	14	14
-1	6	32	30	9	9	27	28	-3	-2	60	57	7	8	18	19	-3	9	40	39	7	6	59	58	-3	-7	67	67	-12	-1	14	14
-1	7	16	16	9	10	22	21	-3	-1	33	30	7	6	17	17	-3	10	27	25	7	9	11	11	-2	-1	10	12	-11	-8	11	11
-1	8	21	21	9	11	12	12	-3	0	109	109	7	6	16	16	-3	11	16	15	7	8	13	13	-2	-3	18	18	-11	-6	14	14
-1	9	21	21	9	12	14	14	-3	0	110	110	7	6	16	16	-3	12	17	17	7	8	13	13	-2	-3	18	18	-11	-6	14	14
-1	10	21	21	9	13	14	14	-3	0	233	233	7	6	16	16	-3	13	18	18	7	8	13	13	-2	-3	18	18	-11	-6	14	14
-1	11	21	21	9	14	14	14	-3	0	234	234	7	6	16	16	-3	14	19	19	7	8	13	13	-2	-3	18	18	-11	-6	14	14
-1	12	21	21	9	15	14	14	-3	0	47	47	7	6	16	16	-3	15	20	20	7	8	13	13	-2	-3	18	18	-11	-6	14	14
-1	13	21	21	9	16	14	14	-3	0	47	47	7	6	16	16	-3	16	21	21	7	8	13	13	-2	-3	18	18	-11	-6	14	14
-1	14	21	21	9	17	14	14	-3	0	47	47	7	6	16	16	-3	17	22	22	7	8	13	13	-2	-3	18	18	-11	-6	14	14
-1	15	21	21	9	18	14	14	-3	0	47	47	7	6	16	16	-3	18	23	23	7	8	13	13	-2	-3	18	18	-11	-6	14	14
-1	16	21	21	9	19	14	14	-3	0	47	47	7	6	16	16	-3	19	24	24	7	8	13	13	-2	-3	18	18	-11	-6	14	14
-1	17	21	21	9	20	14	14	-3	0	47	47	7	6	16	16	-3	20	25	25	7	8	13	13	-2	-3	18	18	-11	-6	14	14
-1	18	21	21	9	21	14	14	-3	0	47	47	7	6	16	16	-3	21	26	26	7	8	13	13	-2	-3	18	18	-11	-6	14	14
-1	19	21	21	9	22	14	14	-3	0	47	47	7	6	16	16	-3	22	27	27	7	8	13	13	-2	-3	18	18	-11	-6	14	14
-1	20	21	21	9	23	14	14	-3	0	47	47	7	6	16	16	-3	23	28	28	7	8	13	13	-2	-3	18	18	-11	-6	14	14
-1	21	21	21	9	24	14	14	-3	0	47	47	7	6	16	16	-3	24	29	29	7	8	13	13	-2	-3	18	18	-11	-6	14	14
-1	22	21	21	9	25	14	14	-3	0	47	47	7	6	16	16	-3	25	30	30	7	8	13	13	-2	-3	18	18	-11	-6	14	14
-1	23	21	21	9	26	14	14	-3	0	47	47	7	6	16	16	-3	26	31	31	7	8	13	13	-2	-3	18	18	-11	-6	14	14
-1	24	21	21	9	27	14	14	-3	0	47	47	7	6	16	16	-3	27	32	32	7	8	13	13	-2	-3	18	18	-11	-6	14	14
-1	25	21	21	9	28	14	14	-3	0	47	47	7	6	16	16	-3	28	33	33	7	8	13	13	-2	-3	18	18	-11	-6	14	14
-1	26	21	21	9	29	14	14	-3	0	47	47	7	6	16	16	-3	29	34	34	7	8	13	13	-2	-3	18	18	-11	-6	14	14
-1	27	21	21	9	30	14	14	-3	0	47	47	7	6	16	16	-3	30	35	35	7	8	13	13	-2	-3	18	18	-11	-6	14	14
-1	28	21	21	9	31	14	14	-3	0	47	47	7	6	16	16	-3	31	36	36	7	8	13	13	-2	-3	18	18	-11	-6	14	14
-1	29	21	21	9	32	14	14	-3	0	47	47	7	6	16	16	-3	32	37	37	7	8	13	13	-2	-3	18	18	-11	-6	14	14
-1	30	21	21	9	33	14	14	-3	0	47	47	7	6	16	16	-3	33	38	38	7	8	13	13	-2	-3	18	18	-11	-6	14	14
-1	31	21	21	9	34	14	14	-3	0	47	47	7	6	16	16	-3	34	39	39	7	8	13	13	-2	-3	18	18	-11	-6	14	14
-1	32	21	21	9	35	14	14	-3	0	47	47	7	6	16	16	-3	35	40	40	7	8	13	13	-2	-3	18	18	-11	-6	14	14
-1	33	21	21	9	36	14	14	-3	0	47	47	7	6	16	16	-3	36	41	41	7	8	13	13	-2	-3	18	18	-11	-6	14	14
-1	34	21	21	9	37	14	14	-3	0	47	47	7	6	16	16	-3	37	42	42	7	8	13	13	-2	-3	18	18	-11	-6	14	14
-1	35	21	21	9	38	14	14	-3	0	47	47	7	6	16	16	-3	38	43	43	7	8	13	13	-2	-3	18	18	-11	-6	14	14
-1	36	21	21	9	39	14	14	-3	0	47	47	7	6	16	16	-3	39	44	44	7	8	13	13	-2	-3	18	18	-11	-6	14	14
-1	37	21	21	9	40	14	14	-3	0	47	47	7	6	16	16	-3	40	45	45	7	8	13	13	-2	-3	18	18	-11	-6	14	14
-1	38	21	21	9	41	14	14	-3	0	47	47	7	6	16	16	-3	41	46	46	7	8	13	13	-2	-3	18	18	-11	-6	14	14
-1	39	21	21	9	42	14	14	-3	0	47	47	7	6	16	16	-3	42	47	47	7	8	13	13	-2	-3	18	18	-11	-6	14	14
-1	40	21	21	9	43	14	14	-3	0	47	47	7	6	16	16	-3	43	48	48	7	8	13	13	-2	-3	18	18	-11	-6	14	14
-1	41	21	21	9	44	14	14	-3	0	47	47	7	6	16	16	-3	44	49	49	7	8	13	13	-2	-3	18	18	-11	-6	14	14
-1	42	21	21	9	45	14	14	-3	0	47	47	7	6	16	16	-3	45	50	50	7	8	13	13	-2	-3	18	18	-11	-6	14	14
-1	43	21	21	9	46	14	14	-3	0	47	47	7	6	16	16	-3	46	51	51	7	8	13	13	-2	-3	18	18	-11	-6	14	14
-1	44	21	21	9	47	14	14	-3	0	47	47	7	6	16	16	-3	47	52	52	7	8	13	13	-2	-3	18	18	-11	-6	14	14
-1	45	21	21	9	48	14	14	-3	0	47	47	7	6	16	16	-3	48	53	53	7	8	13	13	-2	-3	18	18	-11	-6	14	14
-1	46	21	21	9	49	14	14	-3	0	47	47	7	6	16	16	-3	49	54	54	7	8	13	13	-2	-3	18	18	-11	-6	14	14
-1	47	21	21	9	50	14	14	-3	0	47	47	7	6	16	16	-3	50	55	55	7	8	13	13	-2	-3	18	18	-11	-6	14	14
-1	48	21	21	9	51	14	14	-3	0	47	47	7	6	16	16	-3	51	56	56	7	8	13	13	-2	-3	18	18	-11	-6	14	14
-1	49	21	21	9	52	14	14	-3	0	47	47	7	6	16	16	-3	52	57	57	7	8	13	13	-2	-3	18	18	-11	-6	14	14
-1	50	21	21	9	53	14	14	-3	0	47	47	7	6	16	16	-3	53	58	58	7	8	13	13	-2	-3	18	18	-11	-6	14	14
-1	51	21	21	9	54	14	14	-3	0	47	47	7	6	16	16	-3	54	59	59	7	8	13	13	-2	-3	18	18	-11	-6	14	14
-1	52	21	21	9	55	14	14	-3	0	47	47	7	6	16	16	-3	55	60	60	7	8	13	13	-2	-3	18	18	-11	-6	14	14
-1	53	21	21	9	56	14	14	-3	0	47	47	7	6	16	16	-3	56	61	61	7	8	13	13	-2	-3	18	18	-11	-6	14	14
-1	54	21	21	9	57	14	14	-3	0	47	47	7	6	16	16	-3	57	62	62	7	8	13	13	-2	-3	18	18	-11	-6	14	14
-1	55	21	21	9	58	14	14	-3	0	47	47	7	6	16	16	-3	58	63	63	7	8	13	13	-2	-3	18	18	-11	-6	14	14
-1	56	21	21	9	59	14	14	-3	0	47	47	7	6	16	16	-3	59	64	64	7	8	13	13	-2	-3	18	18	-11	-6	14	14
-1	57	21	21	9	60	14	14	-3	0	47	47	7	6	16	16	-3	60	65	65	7	8	13	13	-2	-3	18	18	-11	-6	14	14
-1	58	21																													



and that the true symmetry is  $P1$ . The rather large anisotropic vibration especially in the  $y$ -direction (Table 3) may possibly be due to absorption effects. But divalent and trivalent ions with rather different  $M$ -O distances ( $Fe^{2+}$ -O = 2.17 Å;  $Fe^{3+}$ -O = 2.045 Å;  $Mg^{2+}$ -O = 2.12 Å;  $Al^{3+}$ -O = 1.93 Å according to Shannon and Prewitt, 1969) and very different electron configurations are distributed over twelve octahedral sites in the unit cell, and at least partial order is expected. There are in fact significant differences in refined occupancy factors (Table 6). The smallest  $M(1, 2)$  site has also the smallest occupancy factor and has presumably a high occupancy of Mg and Al. As has been discussed earlier, absorption for the geometry of data collection is most serious for high angle reflections, which thus do not contribute significantly to occupancy factors. Therefore we maintain that the encountered differences are real and not artifacts. Notice also that occupancy factors for isotropic and anisotropic refinements are virtually identical and, although the deviation from unity is only up to five times the estimated error, it seems to be significant. If there is partial order, then order in the octahedral bands would destroy the centrosymmetry. For instance the  $M(2, 2)$  octahedron is related by a center to the directly adjacent octahedron  $M(2, 2C)$ . An attempt to refine the structure in  $P1$  failed because of the high correlation coeffi-

TABLE 2. Atomic Coordinates and Isotropic Temperature Factors for Howieite, Refined in Space Group  $P1^*$

Atom	x	y	z	B
M(1,1)	-0.45599(9)	0.29345(9)	0.23699(9)	0.71(2)
M(1,2)	-0.46434(8)	0.26095(8)	-0.42833(9)	0.48(2)
M(1,3)	-0.46138(9)	0.27582(9)	-0.09654(9)	0.68(2)
M(2,1)	-0.15485(8)	0.42838(8)	0.30607(8)	0.56(2)
M(2,2)	-0.15716(8)	0.42405(8)	-0.36488(9)	0.60(2)
M(2,3)	-0.14897(8)	0.43047(8)	-0.03362(8)	0.46(2)
Na	0	0	0	2.72(12)
Si(1,1)	-0.27392(15)	0.08663(15)	0.01664(16)	0.46(2)
Si(1,2)	-0.27312(15)	0.07690(15)	0.32831(16)	0.48(2)
Si(2,1)	0.00065(15)	0.22071(15)	0.41972(16)	0.45(2)
Si(2,2)	-0.00205(15)	0.21802(15)	-0.26243(16)	0.46(2)
Si(3,1)	0.27037(15)	0.33955(15)	-0.16660(16)	0.45(2)
Si(3,2)	0.27346(15)	0.34722(15)	0.14394(16)	0.53(2)
O(1,1)	0.4140(4)	0.0524(4)	-0.0256(4)	1.05(6)
O(1,2)	0.3627(5)	0.0755(5)	0.3153(5)	1.88(6)
O(1,3)	0.3960(4)	0.0723(4)	-0.4100(4)	0.83(6)
O(2,1)	-0.3179(4)	0.2321(4)	0.0248(4)	0.72(6)
O(2,2)	-0.3285(4)	0.2176(4)	0.3597(4)	0.73(6)
O(2,3)	-0.3408(4)	0.2244(4)	-0.3133(4)	0.88(6)
O(3,1)	-0.0361(4)	0.3832(4)	0.0989(4)	0.75(6)
O(3,2)	-0.0277(4)	0.3742(4)	0.4293(4)	0.74(6)
O(3,3)	-0.0300(4)	0.3714(4)	-0.2481(4)	0.64(6)
O(4,1)	0.2651(4)	-0.4892(4)	0.1604(4)	0.72(6)
O(4,2)	0.2857(4)	-0.4587(4)	0.4857(4)	0.95(6)
O(4,3)	0.2676(4)	-0.4960(4)	-0.1790(4)	0.91(6)
O(5,1)	-0.4313(4)	-0.3249(4)	+0.2404(4)	0.85(6)
O(5,2)	-0.4484(4)	-0.3462(4)	-0.4530(5)	1.36(7)
O(5,3)	-0.4364(4)	-0.3414(4)	-0.1071(4)	0.86(6)
O(6,1)	-0.1288(4)	0.0996(4)	0.3781(4)	0.92(6)
O(6,2)	-0.1342(4)	0.0952(4)	-0.1351(4)	0.81(6)
O(7,1)	0.1601(4)	0.2391(4)	0.2938(4)	0.86(6)
O(7,2)	0.1506(4)	0.2300(4)	-0.2338(4)	0.86(6)
O(8)	-0.2084(4)	0.0703(4)	0.1478(4)	0.74(6)
O(9)	0.0047(4)	0.1631(4)	-0.4239(4)	0.70(6)
O(10)	0.2094(4)	0.2782(4)	0.0107(4)	0.78(6)

\* Estimated error of the least significant digits in this and the following tables is given in parentheses.

icients. But a refinement of just the  $M$  occupancies in  $P1$  produced significant differences in the pseudo-centrosymmetric atoms. A schematic display of the

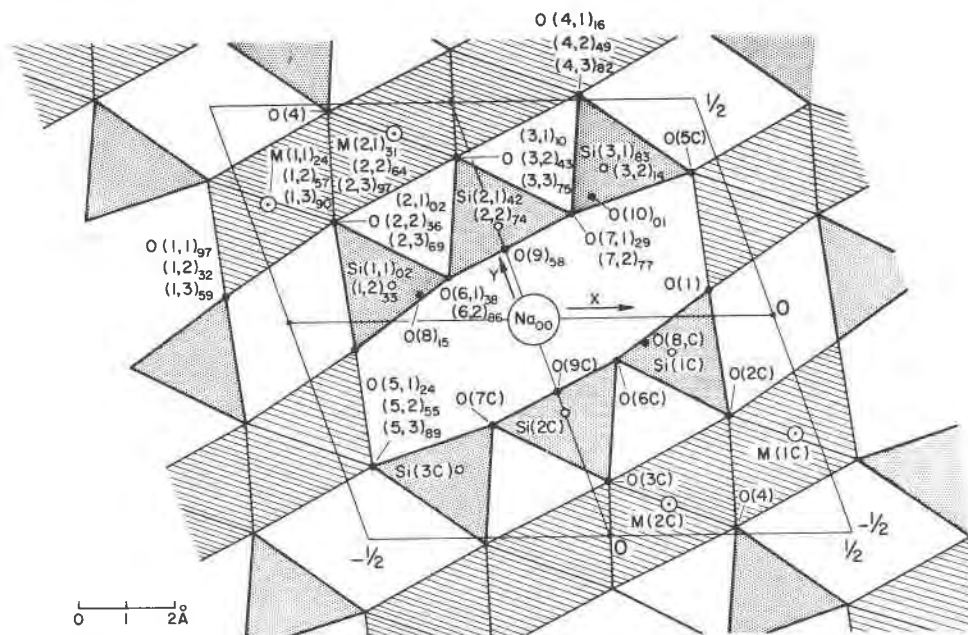


FIG. 4.  $xy$ -projection of the structure of howieite, slightly schematic (atoms in chains along  $z$ -axis are drawn exactly on top of each other).  $z$ -coordinate, rounded to 2 decimals, given as subscript.



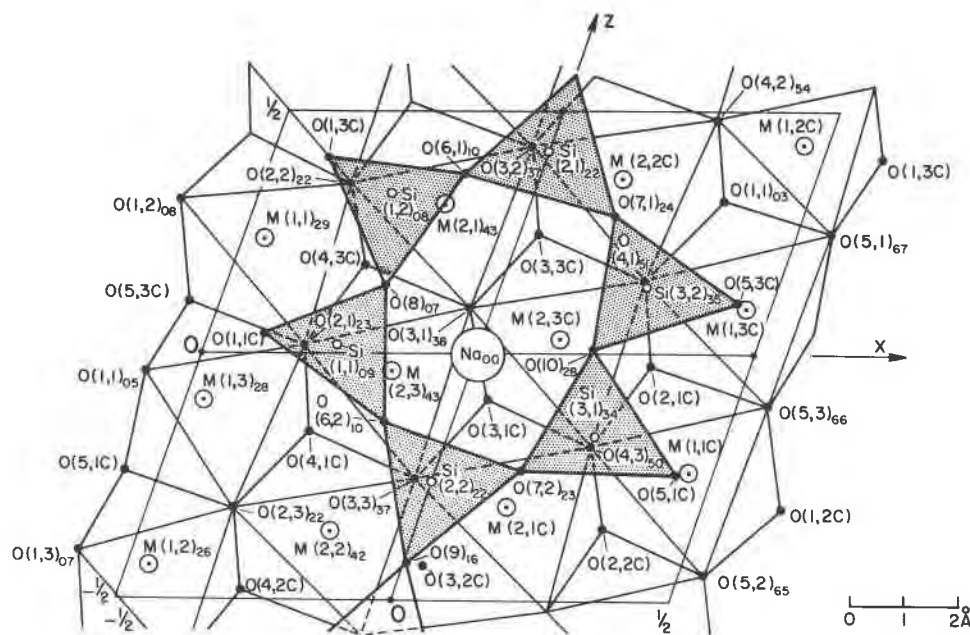


FIG. 5.  $xz$ -projection of the structure of howieite, illustrating the octahedral band (unshaded) with the attached tetrahedral chain (shaded).  $y$ -coordinate rounded to 2 decimals given as subscript. The shaded tetrahedra, whose apices point down, represent the  $[\text{Si}_2\text{O}_7]$  repeat unit of the chain.

TABLE 3. Anisotropic Temperature Factors.  $\beta_{ij}$  of all Atoms in a Centric Refinement of the Howieite Structure\*

	$\beta \times 10^4$					
M(1,1)	155(8)	302(8)	191(9)	87(6)	-72(6)	-5(6)
M(1,2)	101(8)	175(8)	129(8)	48(5)	-26(6)	-11(5)
M(1,3)	160(8)	307(8)	155(8)	106(6)	-38(6)	-18(6)
M(2,1)	121(8)	233(8)	138(9)	50(6)	-22(6)	3(6)
M(2,2)	127(8)	252(8)	154(9)	68(6)	-32(6)	-26(6)
M(2,3)	87(8)	193(8)	132(9)	39(6)	-35(6)	-6(5)
Na	749(52)	1429(66)	756(55)	859(47)	39(39)	306(43)
Si(1,1)	117(12)	183(12)	128(13)	55(9)	-23(10)	9(9)
Si(1,2)	131(12)	219(13)	126(13)	45(10)	-44(10)	-40(10)
Si(2,1)	134(12)	185(12)	127(13)	83(10)	-36(10)	-15(9)
Si(2,2)	136(12)	192(12)	110(13)	72(9)	-46(10)	-19(9)
Si(3,1)	95(12)	222(13)	141(13)	75(10)	-39(10)	-25(10)
Si(3,2)	136(12)	251(13)	122(13)	122(10)	-22(10)	-19(10)
	$\beta \times 10^4$					
O(1,1)	18(3)	34(4)	50(4)	4(3)	-13(3)	-1(3)
O(1,2)	65(5)	41(4)	67(5)	12(4)	-22(4)	5(4)
O(1,3)	22(3)	17(3)	29(4)	0(3)	2(3)	0(3)
O(2,1)	23(3)	18(3)	26(4)	7(3)	-7(3)	7(3)
O(2,2)	19(3)	18(3)	26(4)	8(3)	-2(3)	3(3)
O(2,3)	18(3)	30(3)	27(4)	10(3)	-6(3)	-1(3)
O(3,1)	13(3)	27(3)	26(4)	7(3)	-5(3)	2(3)
O(3,2)	19(3)	25(3)	25(4)	11(3)	-9(3)	-4(3)
O(3,3)	19(3)	21(3)	18(3)	10(3)	-4(3)	+0(3)
O(4,1)	23(3)	29(3)	18(4)	17(3)	-7(3)	-1(3)
O(4,2)	22(3)	38(4)	26(4)	14(3)	-9(3)	-2(3)
O(4,3)	24(3)	28(3)	26(4)	14(3)	-3(3)	-5(3)
O(5,1)	13(3)	35(4)	28(4)	10(3)	-6(3)	-5(3)
O(5,2)	58(4)	57(4)	31(4)	36(4)	-25(4)	-10(3)
O(5,3)	14(3)	34(4)	26(4)	11(3)	-1(3)	4(3)
O(6,1)	25(4)	30(3)	40(4)	10(3)	-24(3)	-5(3)
O(6,2)	19(3)	32(3)	21(4)	8(3)	0(3)	2(3)
O(7,1)	25(3)	35(3)	20(4)	15(3)	-5(3)	-1(3)
O(7,2)	24(3)	33(3)	33(4)	13(3)	-16(3)	-14(3)
O(8)	18(3)	38(3)	20(3)	14(3)	-9(3)	-6(3)
O(9)	29(3)	31(3)	10(3)	16(3)	-5(3)	-2(3)
O(10)	24(3)	37(3)	15(3)	15(3)	-3(3)	-2(3)

\* The form of the thermal ellipsoid is

$$\exp - [\beta_{11}h^2 + \beta_{22}k^2 + \beta_{33}l^2 + 2\beta_{12}hk + 2\beta_{13}hl + 2\beta_{23}kl].$$

TABLE 4. Interatomic Distances and Angles of Tetrahedra in Howieite

	$\text{\AA}$		$\text{\AA}$	corresponding angle O-Si-O
Si(1,1)-O(1,1C)	1.594(4)	O(1,1C)-O(2,1)	2.628(6)	109.8(2)
	-O(2,1)	O(1,1C)-O(6,2)	2.659(6)	111.0(2)
	-O(6,2)	O(1,1C)-O(8)	2.664(6)	110.3(2)
	-O(8)	O(2,1)-O(6,2)	2.700(6)	111.4(2)
average	1.624	O(2,1)-O(8)	2.688(6)	111.7(2)
		O(6,2)-O(8)	2.559(6)	102.4(2)
		average	2.650	109.4
Si(1,2)-O(1,3C)	1.585(4)	O(1,3C)-O(2,2)	2.701(6)	114.0(2)
	-O(2,2)	O(1,3C)-O(6,1)	2.605(6)	107.9(2)
	-O(6,1)	O(1,3C)-O(8)	2.674(6)	111.8(2)
	-O(8)	O(2,2)-O(6,1)	2.694(6)	110.9(2)
average	1.625	O(2,2)-O(8)	2.661(6)	108.4(2)
		O(6,1)-O(8)	2.572(6)	103.3(2)
		average	2.651	109.4
Si(2,1)-O(3,2)	1.613(4)	O(3,2)-O(6,1)	2.640(5)	109.9(2)
	-O(6,1)	O(3,2)-O(7,1)	2.650(6)	109.7(2)
	-O(7,1)	O(3,2)-O(9)	2.687(5)	111.9(2)
	-O(9)	O(6,1)-O(7,1)	2.647(6)	109.6(2)
average	1.621	O(6,1)-O(9)	2.633(6)	108.5(2)
		O(7,1)-O(9)	2.622(6)	107.2(2)
		average	2.647	109.5
Si(2,2)-O(3,3)	1.610(4)	O(3,3)-O(6,2)	2.661(5)	110.3(2)
	-O(6,2)	O(3,3)-O(7,2)	2.672(5)	111.0(2)
	-O(7,2)	O(3,3)-O(9)	2.654(5)	110.8(2)
	-O(9)	O(6,2)-O(7,2)	2.602(6)	105.8(2)
average	1.622	O(6,2)-O(9)	2.645(6)	109.0(2)
		O(7,2)-O(9)	2.655(6)	109.8(2)
		average	2.648	109.5
Si(3,1)-O(4,3)	1.624(4)	O(4,3)-O(5,1C)	2.720(6)	114.6(2)
	-O(5,1C)	O(4,3)-O(7,2)	2.670(6)	109.9(2)
	-O(7,2)	O(4,3)-O(10)	2.671(6)	109.1(2)
	-O(10)	O(5,1C)-O(7,2)	2.678(6)	111.2(2)
average	1.631	O(5,1C)-O(10)	2.626(6)	107.1(2)
		O(7,2)-O(10)	2.602(6)	104.4(2)
		average	2.661	109.4
Si(3,2)-O(4,1)	1.630(4)	O(4,1)-O(5,3C)	2.702(5)	113.7(2)
	-O(5,3C)	O(4,1)-O(7,1)	2.686(6)	110.5(2)
	-O(7,1)	O(4,1)-O(10)	2.665(5)	108.5(2)
	-O(10)	O(5,3C)-O(7,1)	2.650(6)	110.0(2)
average	1.630	O(5,3C)-O(10)	2.648(5)	109.1(2)
		O(7,1)-O(10)	2.605(5)	104.6(2)
		average	2.659	109.4

TABLE 5. Interatomic Distances and Angles of Octahedra in Howieite

	$\bar{d}$		$\bar{d}$	corresponding angle O-M-O
M(1,1)-O(1,2)	2.256(4)	0(1,2)-O(2,1)	3.409(7)	98.2(2)
-O(2,1)	2.256(5)	0(1,2)-O(2,2)	3.158(6)	87.8(2)
-O(2,2)	2.300(4)	0(1,2)-O(5,2C)	2.933(6)	84.3(2)
-O(4,3C)	2.183(4)	0(1,2)-O(5,3C)	3.044(6)	89.7(2)
-O(5,2C)	2.111(5)	0(2,1)-O(2,2)	3.182(5)	88.6(1)
-O(5,3C)	2.056(4)	0(2,1)-O(4,3C)*	2.929(6)	82.6(2)
average	2.194	0(2,1)-O(5,3C)*	2.902(6)	84.5(1)
		0(2,2)-O(4,3C)*	3.031(6)	85.0(1)
		0(2,2)-O(5,2C)*	2.830(6)	79.7(2)
		0(4,3C)-O(5,2C)	3.129(6)	93.5(2)
		0(4,3C)-O(5,3C)	3.189(6)	97.5(2)
		0(5,2C)-O(5,3C)	3.358(6)	107.4(2)
		average	3.091	89.9
M(1,2)-O(1,3)	1.894(4)	0(1,3)-O(2,2)	2.701(6)	89.3(2)
-O(2,2)	2.172(4)	0(1,3)-O(2,3)	3.035(6)	101.0(2)
-O(2,3)	2.036(4)	0(1,3)-O(5,1C)	2.917(6)	97.9(2)
-O(4,2C)	2.105(4)	0(1,3)-O(5,2C)	2.816(6)	92.9(2)
-O(5,1C)	1.972(4)	0(2,2)-O(2,3)	3.096(5)	94.7(2)
-O(5,2C)	1.992(4)	0(2,2)-O(4,2C)*	2.748(6)	79.9(2)
average	2.029	0(2,2)-O(5,2C)*	2.830(6)	85.6(2)
		0(2,3)-O(4,2C)*	2.646(6)	79.4(2)
		0(2,3)-O(5,1C)	2.686(6)	84.1(2)
		0(4,2C)-O(5,1C)	2.955(6)	92.8(2)
		0(4,2C)-O(5,2C)	2.819(6)	86.9(2)
		0(5,1C)-O(5,2C)	2.896(6)	93.9(2)
		average	2.845	89.9
M(1,3)-O(1,1)	2.126(4)	0(1,1)-O(2,1)	2.628(6)	82.4(2)
-O(2,1)	2.283(4)	0(1,1)-O(2,3)	3.095(6)	91.8(2)
-O(2,3)	2.181(4)	0(1,1)-O(5,1C)	3.324(6)	101.6(2)
-O(4,1C)	2.289(4)	0(1,1)-O(5,3C)	3.044(6)	92.6(2)
-O(5,1C)	2.164(4)	0(2,1)-O(2,3)	3.324(5)	96.2(1)
-O(5,3C)	2.086(4)	0(2,1)-O(4,1C)*	2.905(6)	78.9(1)
average	2.188	0(2,1)-O(5,3C)*	2.902(6)	83.1(1)
		0(2,3)-O(4,1C)*	2.954(6)	82.7(2)
		0(2,3)-O(5,1C)	2.686(6)	76.4(2)
		0(4,1C)-O(5,1C)	3.311(6)	96.0(1)
		0(4,1C)-O(5,3C)	3.169(6)	92.7(2)
		0(5,1C)-O(5,3C)	3.349(5)	104.0(2)
		average	3.058	89.9
M(2,1)-O(2,2)	2.167(4)	0(2,2)-O(3,1)	3.137(6)	95.2(2)
-O(3,1)	2.081(4)	0(2,2)-O(3,2)*	3.223(5)	95.2(1)
-O(3,2)	2.198(4)	0(2,2)-O(4,2C)*	2.748(6)	80.6(2)
-O(3,3C)	2.150(4)	0(2,2)-O(4,3C)	3.031(6)	88.8(2)
-O(4,2C)	2.080(4)	0(3,1)-O(3,2)*	2.742(8)	96.8(2)
-O(4,3C)	2.165(4)	0(3,1)-O(3,3C)*	2.772(6)	81.8(2)
average	2.140	0(3,1)-O(4,3C)*	2.796(6)	82.4(2)
		0(3,2)-O(3,3C)*	2.847(6)	81.8(1)
		0(3,2)-O(4,2C)	2.865(6)	84.0(2)
		0(3,3C)-O(4,2C)	3.297(6)	102.4(2)
		0(3,3C)-O(4,3C)	3.161(5)	94.2(2)
		0(4,2C)-O(4,3C)	3.181(6)	97.1(2)
		average	2.983	90.0
M(2,2)-O(2,3)	2.142(4)	0(2,3)-O(3,2)	3.209(6)	97.4(2)
-O(3,2)	2.129(4)	0(2,3)-O(3,3)*	3.278(5)	99.7(2)
-O(3,3)	2.146(4)	0(2,3)-O(4,1C)*	2.954(6)	88.1(2)
-O(3,2C)	2.160(4)	0(2,3)-O(4,2C)	2.646(6)	76.9(2)
-O(4,1C)	2.108(4)	0(3,2)-O(3,3)	3.086(5)	92.4(2)
-O(4,2C)	2.114(4)	0(3,2)-O(3,2C)*	2.768(8)	80.4(2)
average	2.133	0(3,2)-O(4,2C)*	2.865(6)	85.0(2)
		0(3,3)-O(3,2C)*	2.847(6)	82.8(1)
		0(3,3)-O(4,1C)	2.861(6)	84.5(1)
		0(3,2C)-O(4,1C)	3.128(6)	94.3(2)
		0(3,2C)-O(4,2C)	3.288(6)	100.6(2)
		0(4,1C)-O(4,2C)	3.196(6)	98.4(2)
		average	3.011	90.0
M(2,3)-O(2,1)	2.064(4)	0(2,1)-O(3,1)	3.071(5)	94.5(2)
-O(3,1)	2.116(4)	0(2,1)-O(3,3)*	3.126(6)	94.6(2)
-O(3,3)	2.190(4)	0(2,1)-O(4,1C)*	2.905(6)	87.1(2)
-O(3,1C)	2.069(4)	0(2,1)-O(4,3C)	2.929(6)	86.6(2)
-O(4,1C)	2.149(4)	0(3,1)-O(3,3)*	3.307(5)	81.2(2)
-O(4,3C)	2.203(4)	0(3,1)-O(3,1C)*	2.742(8)	81.8(2)
average	2.132	0(3,1)-O(4,3C)*	2.796(6)	80.7(2)
		0(3,3)-O(3,1C)*	2.772(6)	81.2(2)
		0(3,3)-O(4,1C)*	2.861(6)	82.5(1)
		0(3,1C)-O(4,1C)	3.153(5)	96.7(2)
		0(3,1C)-O(4,3C)	3.218(6)	97.7(2)
		0(4,1C)-O(4,3C)	3.245(5)	96.4(2)
		average	3.010	88.4
M(1,1)-M(1,2)	3.202(2)	M(2,1)-M(2,2)	3.149(2)	
M(1,1)-M(1,3)	3.217(2)	M(2,1)-M(2,3)	3.213(2)	
M(1,1)-M(2,1)	3.196(2)	M(2,1)-M(2,2)	3.259(2)	
M(1,1)-M(2,3)	3.217(1)	M(2,1)-M(2,3C)	3.238(2)	
M(1,2)-M(1,3)	3.191(2)	M(2,2)-M(2,3)	3.204(2)	
M(1,2)-M(2,1)	3.255(3)	M(2,2)-M(2,1C)	3.259(2)	
M(1,2)-M(2,2)	3.260(2)	M(2,2)-M(2,2C)	3.277(2)	
M(1,3)-M(2,2)	3.205(3)	M(2,3)-M(2,1C)	3.213(3)	
M(1,3)-M(2,3)	3.290(2)	M(2,3)-M(2,3C)	3.162(2)	
average distance			3.223	

\* indicates shared edges.

TABLE 6. Occupancy Factors for M and Na Positions in Howieite\*

	Centric Refinement		Acentric Refinement, isotropic	
	isotropic	anisotropic	only 12 M-occupancies refined	12 M-occupancies and 30 O-positions refined
R <sub>2</sub>	7.79%	6.18%	7.76%	7.63%
M(1,1)	.998(5)	.997(4)	.991(11)	.994(11)
M(1,1C)			1.000(11)	.990(11)
M(1,2)			.884(10)	.894(10)
M(1,2C)	.980(5)	.978(4)	1.077(10)	1.061(11)
M(1,3)			1.081(11)	1.073(11)
M(1,3C)	.999(5)	.999(4)	.912(11)	.912(11)
M(2,1)			.962(10)	.975(10)
M(2,1C)	1.022(5)	1.026(4)	1.081(10)	1.059(10)
M(2,2)			.959(11)	.957(10)
M(2,2C)	1.005(5)	1.006(4)	1.051(11)	1.045(11)
M(2,3)			.955(10)	.974(11)
M(2,3C)	1.028(5)	1.030(4)	1.035(10)	1.007(11)
Na	.933(16)	.946(13)	.933	.933

\* Compare Figure 8.

occupancies over the twelve M-sites is shown in Figure 8. As can be seen, high and low occupancies do not seem to be simply alternating. These symmetry considerations cannot be satisfactorily resolved with X-ray data. Unambiguous proof for noncentric structure would have to come from more sensitive methods such as magnetic resonance studies.

The structural and chemical formula derived from

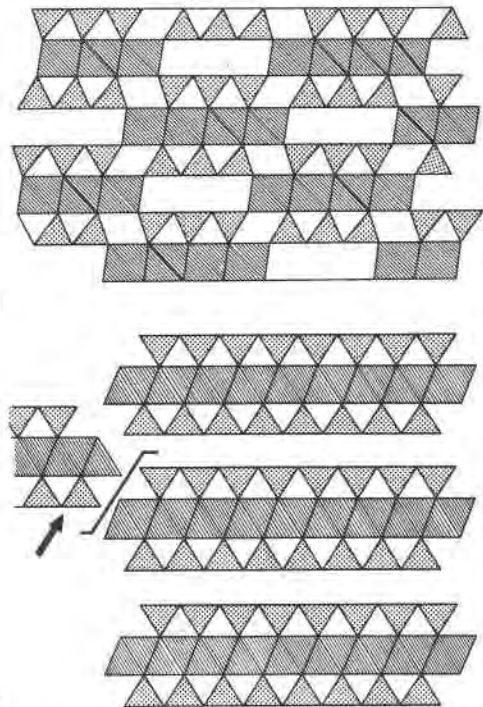


FIG. 6. a. Schematic diagram comparing the howieite structure (a) with a sheet silicate structure. b. z-projection in howieite, y-projection in sheet silicate (mica setting).

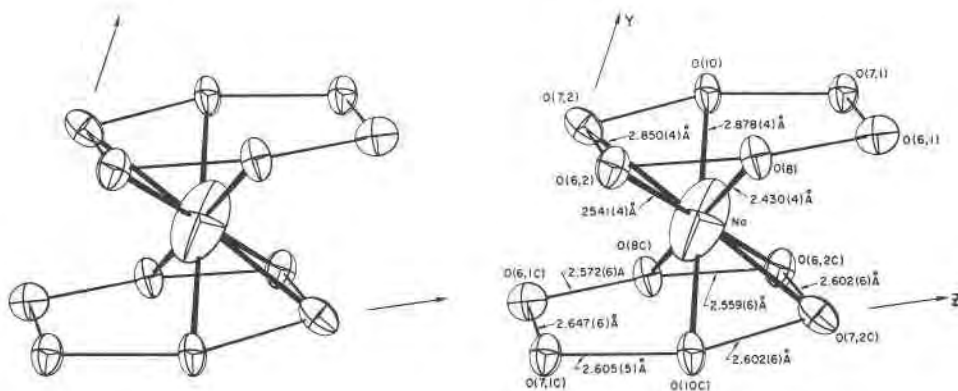


FIG. 7. Stereoscopic pair of drawings displaying the coordination of Na in the howieite structure. View is along  $x$ . Ellipsoids give 95 percent probability contour of thermal vibration.

the structure determination is  $\text{Na}(\text{Fe}^{2+}, \text{Mg}, \text{Fe}^{3+}, \text{Al})_{12} [\text{Si}_6\text{O}_{17}]_2, [\text{O}, \text{OH}]_{10}$ . To achieve a charge balance, at least 10 of the 44 oxygens—presumably the free tetrahedral corners of the  $[\text{Si}_6\text{O}_{17}]$ -chain as well as some octahedral anions—must be  $\text{OH}^-$ .

The structural building unit of howieite is the octahedral band which is decorated on both sides

with a  $[\text{Si}_6\text{O}_{17}]$ -chain. This chain is intermediate between a double and a single chain. Therefore howieite resembles an amphibole or a pyroxene. But it is easier to relate it to sheet silicates. This is illustrated in Figure 6 which compares a  $z$ -projection of howieite with a  $y$ -projection of a sheet silicate (mica setting). The stacking sequence in both of them consists of an octahedral layer, a tetrahedral layer, and between two tetrahedral layers a highly coordinated large cation site. In howieite this site is mainly occupied by Na. The site which has 12-fold coordination in the ideal structure is distorted such that each Na has only 8 oxygens as closest neighbors (Figure 7). The “sheetplane” (001) in sheet silicates (Figure 6b) is (120) in howieite (Figure 6a). In contrast to sheet silicates, the layers do not extend indefinitely but are interrupted after four rows of octahedra and a second set of “sheet units” is inserted with a displacement  $\sim 1/6 x$  and  $1/2 y$  resulting in an intricate linkage resembling a brick-frame. Octahedral units partially occupy the loosely packed large cation layers and therefore the howieite structure is denser than an ordinary sheet silicate with more  $M$  and less Si and Na in the corresponding formula unit [glaucosite:  $[\text{Na}_4\text{M}_{12}\text{Si}_6(\text{O}, \text{OH})_{48}, V = 947 \text{ \AA}^3, \rho = 2.4$  to  $2.45 \text{ g/cc}$ ; howieite:  $\text{NaM}_{12}\text{Si}_{12}(\text{O}, \text{OH})_{44}, V = 851 \text{ \AA}^3, \rho = 3.38 \text{ g/cc}$ ]. Howieite may be the high-pressure breakdown product of a sheet silicate. Its formation can be plausibly expected to be favored by shearing under high confining pressure, conditions which most likely prevailed in the metamorphic recrystallization of the Franciscan formation in California.

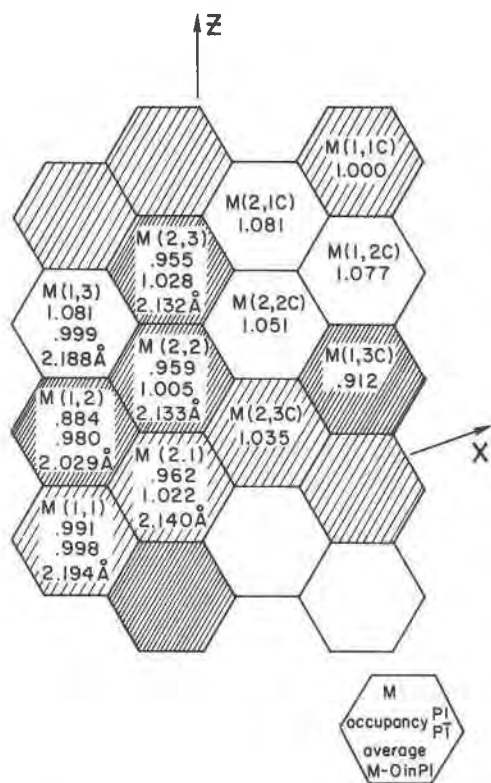


FIG. 8. Variation of occupancy factors and average  $M$ -O distance in the 12  $M$  positions (compare also Table 6) (schematic  $xz$ -projection). Shading indicates octahedra of high, medium, and low occupancy.

Howieite resembles and has been mistaken for stilpnomelane which occurs with it. It is most readily distinguished by its inclined extinction; otherwise

optical properties are similar. The rather unstable structure of stilpnomelane (Eggleton, 1972) with warping sheets of octahedral cations can indeed be visualized as some intermediate state between a stable sheet silicate and howieite. A rewarding project for investigation will be the stability field of howieite and possibly breakdown reactions, especially in comparison to the structurally related coexisting minerals, stilpnomelane, amphibole, and deerite which form this interesting high-pressure, low-temperature assemblage in the Franciscan formation.

### Acknowledgments

The mineral was collected on a field trip with Dr. S. Agrell. The data set was collected on the Picker diffractometer at the Lawrence Berkeley Laboratory through the courtesy of Dr. A. Zalkin. Mr. D. Greig assisted in the initial data processing. I acknowledge the help of Dr. S. Goldberg and Ms E. N. Duesler in questions of computer programs, and the stimulating discussions with Dr. S. Ghose and Professor D. Templeton. The calculations were done partially on the CDC 6400 computer on the Berkeley campus, partially on the CDC 7600 of the Lawrence Berkeley Laboratory.

### References

- AGRELL, S. O., M. G. BOWN, AND D. MCKIE (1965) Deerite, howieite, and zussmanite, three new minerals from the Franciscan of the Laytonville district, Mendocino County, California. *Amer. Mineral.* **50**, 278.
- BUSING, W. R., K. O. MARTIN, AND H. A. LEVY (1962) A FORTRAN crystallographic function and error program. *U. S. Nat. Tech. Inform. Serv.* ORNL-TM-308.
- CORFIELD, P. W. R., R. J. DOEDENS, AND J. A. IBERS (1967) Studies of metal-nitrogen multiple bonds. I. The crystal and molecular structure of nitridodichlorotris (diethylphenylphosphene) rhenium (V),  $\text{ReNCl}_2[\text{P}(\text{C}_2\text{H}_5)_2\text{C}_6\text{H}_5]_3$ . *Inorg. Chem.* **6**, 197-204.
- CROMER, D. T. (1965) Anomalous dispersion corrections computed from self-consistent field relativistic Dirac-Slater wave functions. *Acta Crystallogr.* **18**, 17-23.
- , AND J. MANN (1968) X-ray scattering factors computed from numerical Hartree-Fock wave functions. *Acta Crystallogr. A* **24**, 321-324.
- DUESLER, E. N., AND K. N. RAYMOND (1971) Conformational effects of intermolecular interactions. The structure of tris-(ethylene diamine) cobalt (III) monohydrogen phosphate nonohydrate. *Inorg. Chem.* **10**, 1486-1492.
- EGGLETON, R. A. (1972) The crystal structure of stilpnomelane. Part II. The full cell. *Mineral. Mag.* **38**, 693-711.
- SHANNON, R. D., AND C. T. PREWITT (1969) Effective ionic radii in oxides and fluorides. *Acta Crystallogr.* **B25**, 925-946.
- WENK, H. R. (1973) The crystal structure of howieite. *Naturwissenschaften*, **60**, 254-255.
- ZACHARIASEN, W. H. (1968) TeMe: Experimental tests of the general formula for the integrated intensity of real crystals. *Acta Crystallogr. A* **24**, 212.

*Manuscript received, June 21, 1973; accepted for publication, October 8, 1973.*